Journal of Hydroscience and Hydraulic Engineering
Vol. 15, No. 1, June, 1997, 55-64

AN OBSERVATION OF THE CLIMATIC EFFECT OF WATERING ON PAVED ROADS

By

Tsuyoshi KINOUCHI

Urban River Division, River Department, Public Works Research Institute,
Asahi 1, Tsukuba, Ibaraki, Japan 305

Manabu KANDA

Department of International Development Engineering, Tokyo Institute of Technology,
O-okayama, Meguro-ku, Tokyo, Japan 152

Minoru KURIKI and Hiroaki KOBAYASHI

Urban River Division, River Department, Public Works Research Institute

SYNOPSIS

Heat environments in growing cities have been deteriorating due to artificial ground cover and anthropogenic heat. The authors focused on the watering of paved roads as an effective and feasible measure against the situation and observed its effect on the micro-climate of urban areas. The results showed that the differences in air temperature, globe temperature and relative humidity at two sites with and without watering were a maximum 1 degrees, 4 degrees and 4%, respectively. In addition, the estimated energy balance at the sites showed that considerable latent heat and lateral heat transport contributed to lowering the surface temperature of a paved road.

INTRODUCTION

In recent years, cities have been increasingly experiencing the so-called "heat island" phenomenon, in which urban temperatures become higher than those in peripheral areas. A rise in temperature produces undesirable situations, e.g., increasing energy consumption as a result of the use of air-conditioners.

Measures that produce an effect for moderating such an urban climate include watering of the ground surface. Although research has already sought to clarify the effect of watering on the heat balance through experiments and numerical analysis[1)], no research has yet entered the phase of field measurement. Accordingly, the authors conducted test watering of the surfaces of roadways in Nagaoka City using watering pipes installed underground in the center of roadways for melting snow, and observed the resulting temperature and humidity to examine the effectiveness of watering as a measure for moderating urban climate. This paper reports on the results of this field study.

OBSERVATION METHODS

The field study was conducted on August 13, 1993, from 9 a.m. until 3 p.m. The weather was unstable. It had been drizzling intermittently until the evening of the previous day. On the day of observation, a low temperature forecast was issued. Although it was fine all morning, it became cloudy in the afternoon. Figure 1 shows the area selected for the observation. Two observation sites were set up, one within the area to be watered (Site A) and the other about 30 m away from this area (Site

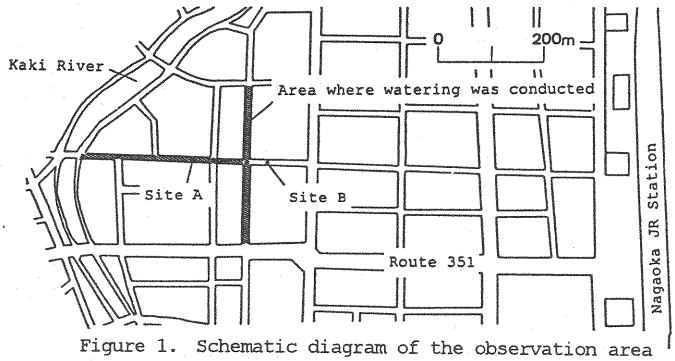

Figure 1. Schematic diagram of the observation area

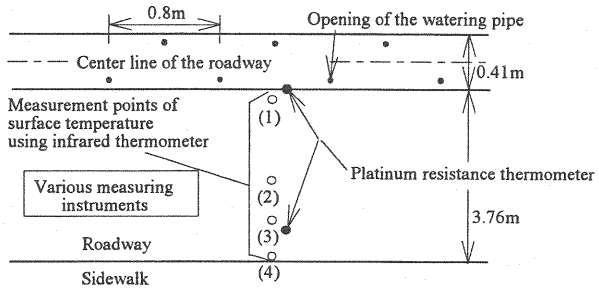

Figure 2. Plane view of Site A

B). For the watering conducted in the field study, the authors used about 500 m of total length of the city's snow-melting pipe network.

Watering was conducted in the area indicated by the oblique lines in Figure 1, from 10 a.m. until 2 p.m.; however, no watering was conducted for one hour after the commencement and one hour prior to the termination of the observation. Measuring instruments were installed at about 1 m above the ground to measure the energy balance of the ground surface, air temperature, globe temperature, relative humidity, and wind velocity. The arrangement of the measuring instruments is shown in Table 1. Site A was equipped with the instrumentation shown schematically in Figure 2. In addition to the items shown in Table 1, wind direction was recorded, and the quantity and temperature of water sprinkled from one opening of the watering pipe were measured.

Table 1. Arrangement of measuring instruments

Both Sites A and B	Measuring instruments	Accuracy	Measurement intervals
Air temperature and relative humidity	Platinum-resistance thermometer Capacitive	VAISALA, IMP130Y ±0.2°C, ±2%RH	10 s
Globe temperature	Platinum-resistance thermometer	±0.2°C	10 s
Wind velocity	3-cup anemometer	-0.3 m/s (not greater than 3 m/s)	10 s
Net radiation Downward short-wave and long-wave radiation	Net radiometer	EKO MF-11 5%	1 s
Heat flux into the ground	Heat flowmeter	EKO MF-81	1 s
Solar radiation	Pyrheliometer	Ishikawa Industries, ±1.5%	1 s
Temperature on the ground surface	Infrared thermometer	Minolta, IR-0510 (emissivity = 1)	Intermittent
Site A exclusively	**Measuring instruments**	**Accuracy**	**Measurement intervals**
Wind velocity, air temperature	Ultrasonic anemometer	±1cm/s, ±0.05°C	2-minute average
Temperature of the sprinkled water	Platinum-resistance thermometer	±0.2°C	10 s

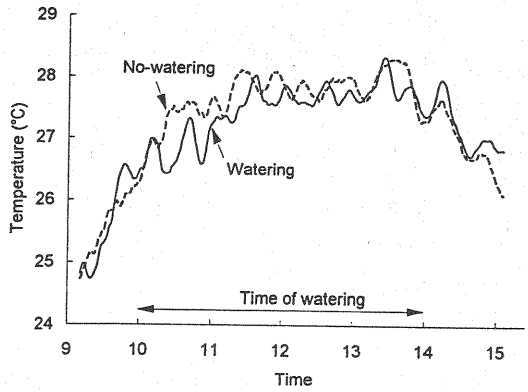

Figure 3. Time distribution of air temperature

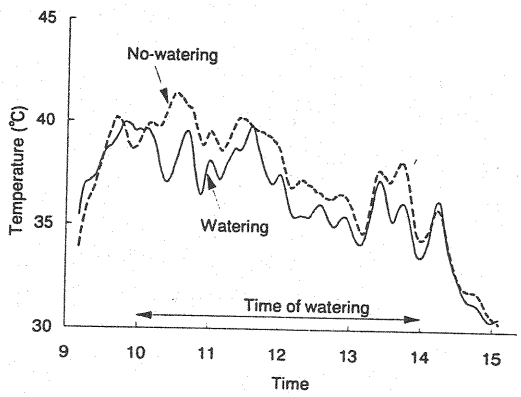

Figure 4. Time distribution of globe temperature

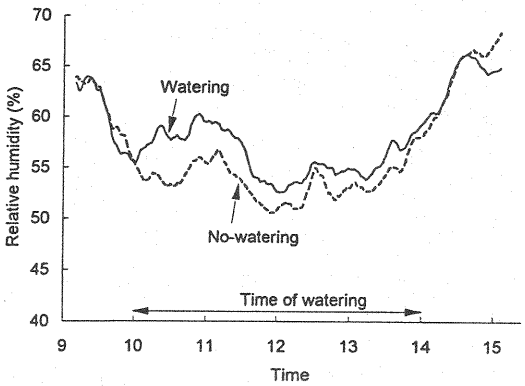

Figure 5. Time distribution of relative humidity

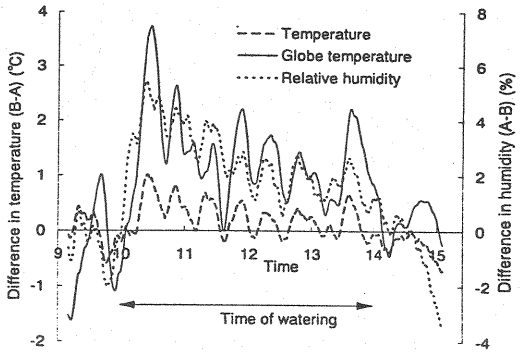

Figure 6. Effect of watering on temperature and humidity

RESULTS OF THE OBSERVATION

Air temperature, globe temperature and relative humidity

The graphs shown in Figures 3, 4, 5 and 6 are the time distribution of air temperature, globe temperature and relative humidity measured at Sites A and B expressed by ten-minute mean, as well as the differences in temperature and humidity between the two sites. On the day of the observation, a wind with a mean velocity of 0.5~2.5 m/s, blowing from Site A to Site B, was predominant. Thus, the watering is considered to have affected the air over Site B. Despite this wind, however, the average temperature measured at Site B was higher than that at Site A by about 0.5 degrees during the time of watering (10:00 a.m. to 2:00 p.m.). Between 10:30 a.m. and 11:30 a.m., when the solar radiation was the greatest, the difference in temperature amounted to a maximum of about 1.0 degrees. On the other hand, the average humidity measured at Site A was higher than that at Site B by several percentage points during the time of watering, showing the maximum difference by about 4%. According to the measurements taken during the two intervals when watering was not conducted, the difference in both temperature and humidity between the two sites either averaged 0, or the temperature was much higher and the humidity lower at Site A. Thus, it can be concluded that the temperature and humidity measured during the time of watering were affected greatly by the watering.

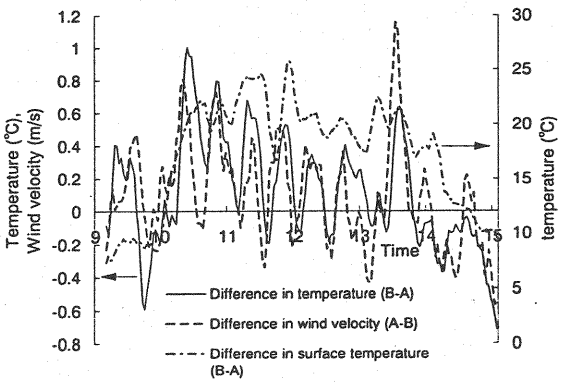

Figure 7. Effect of watering on temperature and wind velocity

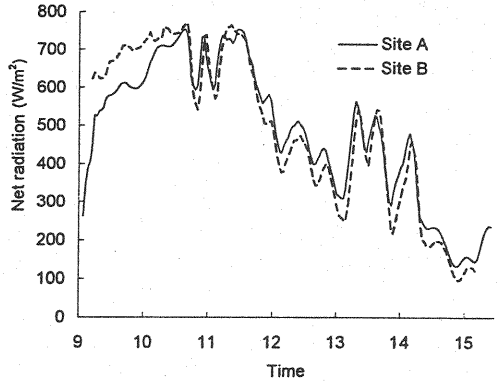

Figure 8. Time distribution of net radiation

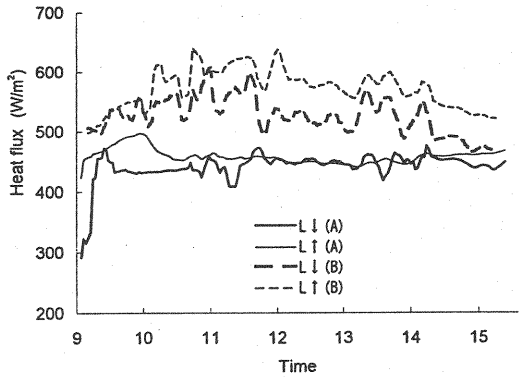

Figure 9. Time distribution of longwave radiation

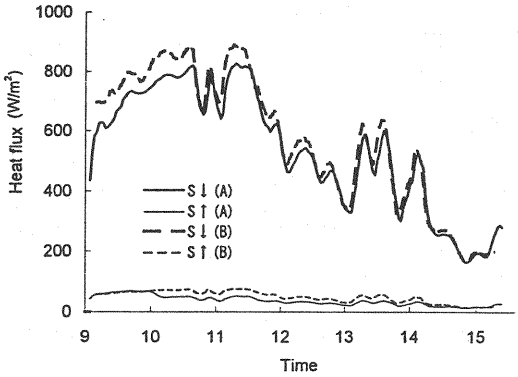

Figure 10. Time distribution of shortwave radiation

Thermal sensation of humans is affected not only by temperature and humidity but also by winds and radiative flux. Similarly, the globe temperature varies depending on the existence of surrounding substances and/or their surface temperature, even if the air temperature and humidity are constant. The differences in globe temperature between Site A and B were conspicuous during the watering. It reached about 4 degrees when the solar radiation was maximum(Figure 6). The low globe temperature at Site A was attributed mostly to the fact that the temperature on the surface of the roadway was lowered by the water distribution as will be shown later.

Figure 7 shows the time distribution of the differences in air temperature, wind velocity and the ground surface temperature between the two sites. The ground surface temperature was obtained from eq.(1). This result indicates that both air temperature and wind velocity fluctuated periodically, and that there was a strong correlation between them. We can see from Figure 7 that the time variation of the difference in the ground surface temperature corresponds to those in air temperature and wind velocity.

Radiation

Figure 8, 9 and 10 show the time variation of the net radiation, long-wave radiation and short-wave radiation, respectively. It must be noted that Site A, constituting a canopy, was more built-up than Site B; thus, downward radiation at Site A was smaller than that at Site B. In addition, upward short-wave radiation at Site A was smaller than that at Site B after the commencement of watering, since watering produced a thin water layer.

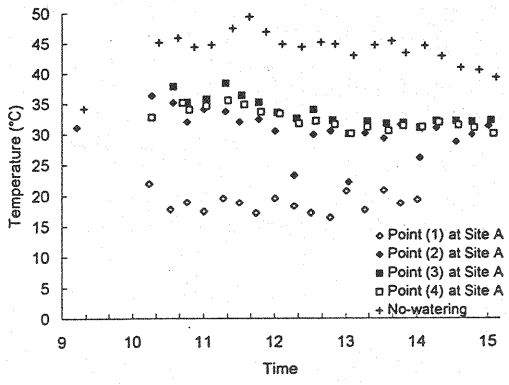

Figure 11. Surface temperature taken with a infrared thermometer

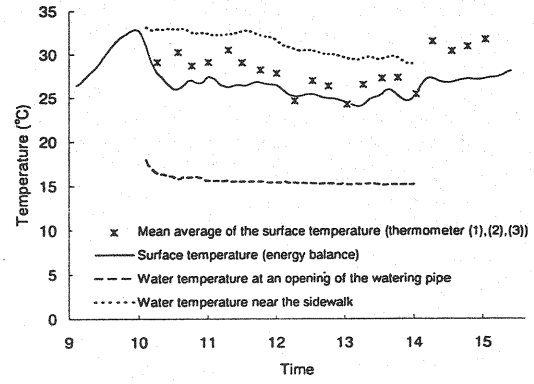

Figure 12. Estimated surface temperature (Site A)

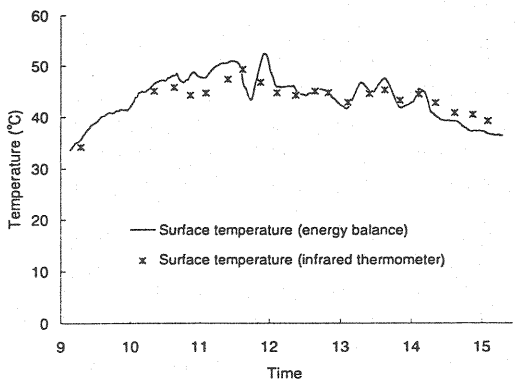

Figure 13. Estimated surface temperature (Site B)

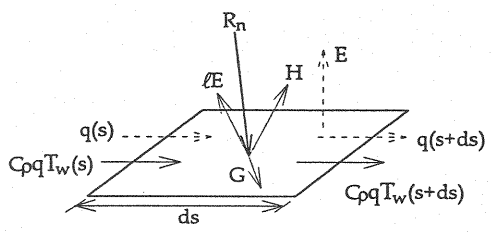

Figure 14. Energy and water balance on a roadway surface with sprinkled water

Ground surface temperature

Figure 11 shows the ground surface temperature measured at both Sites A and B using a infrared thermometer. Measurement was conducted at four different points within Site A between the center of the roadway and the edge of the sidewalk (Figure 2). The ground surface temperature varied as the water flowed into a gutter. The maximum temperature at Site B reached 50 degrees, while that at Site A was lower by 10 to 30 degrees. Figures 12 and 13 compare the ground surface temperature obtained by the infrared thermometer with that calculated from the following equation using measured radiative fluxes:

$$R_n = S\downarrow - S\uparrow + L\downarrow - \sigma T^4 \qquad (1)$$

where $S\downarrow$ is the downward short-wave radiation, $S\uparrow$ is the upward short-wave radiation, $L\downarrow$ is the downward long-wave radiation, σ is the Stefan-Boltzmann constant, and T is the ground surface temperature.

The calculated and measured values were almost identical at Site B, while they were slightly different at Site A. This may be attributed to the fact that the values obtained by eq.(1) are mean values in a certain region, while those obtained by measurement using a radiation thermometer are values within a limited region. Another plausible reason for this may be the uneven wetness of the road surface.

Energy balance

In no-watering area, the net radiation is distributed into heat flux into the ground

and convection of sensible heat. On the other hand, in watering area , the watering increases the partition of the net radiation into latent heat. Moreover, the sprinkled water itself absorbs heat energy as it flows into street drains. Since groundwater was pumped up and used for the watering with the temperature of the sprinkled water being a stable 15 degrees, the effect of advection was considerable, as will be discussed later in this paper.

As shown in Figure 14, the energy balance equation for the surface of an asphalt-paved roadway and the continuity equation for watering are expressed as follows:

$$R_n = G + H + \ell E + c\rho \frac{d(qT_w)}{ds} \quad \text{(Watering)} \tag{2}$$

$$R_n = G + H \quad \text{(No watering)} \tag{3}$$

$$\frac{dq}{ds} = -E \tag{4}$$

where R_n is the net radiation, G is the heat flux into the ground, H is the sensible heat flux into the atmosphere, ℓE is the latent heat flux into the atmosphere, E is the rate of evaporation, q is the discharge per unit width, T_w is the water temperature, $c\rho$ is the heat capacity of water, and s is the distance along the flow direction of sprinkled water.

The energy balance at Site A was calculated in the following manner. Disregarding the variation of q in eq. (2), the heat advection, i.e., the last term in the right-hand side of eq. (2), was estimated using both the water temperature measured with a platinum resistance thermometer at the center of the roadway and near the street drains, and the water discharge measured at one opening of the watering pipe (almost invariably 13.1 $cm^3/s/m$). These estimates ranged from 250 to 310 W/m^2 (Figure 15). The sensible heat was obtained using a ultrasonic anemometer. In this study, a 4 mm-thick heat flowmeter that was originally designed for laying underground, was put on the road surface and covered with adhesive tape. Therefore, the measured values of heat flux into the ground, G, were very low. Given that the energy balance at Site A between 9:00 a.m. and 10:00 a.m., when the watering was not conducted, is in conformity with eq. (3), the values of G obtained by measurement were corrected to comply with the condition E=O. The values used for this correction were the temperature on the lower face of the heat flowmeter(which was estimated using the energy balance equation for the upper face of the heat flowmeter, and the measured values of the radiation and G), the calculated values of the temperature of the road surface and the sensitivity constant and thermal resistance of the heat flowmeter.

Figure 15 shows the time distribution of both the corrected values of G and the values of each term in eq. (2) expressed in 10-minute averages. Since the temperature on the road surface decreased sharply just after the watering, the conductive heat flux into the ground "nose-dived" to negative values, while the values of latent heat flux increased (Figure 17). Later, however, the latent heat flux gradually decreased. This is corroborated by the gradual decrease in the difference in humidity between Sites A and B (Figure 6). It should be noted that the sudden decline in the value of G at around 9:30 a.m. and the appearance of a latent heat transport may have been caused by preliminary watering conducted for several minutes at that time.

The values of sensible and latent heat flux at Site A were respectively compared with those estimated by the gradient method (Figures 16 and 17). Concerning the measured values of sensible heat flux, no abrupt decrease due to the commencement of watering was observed. Although the measured values of sensible heat became negative around 1:00 p.m., they were higher than the estimated values by several tens of w/m^2 after the watering. Concerning the latent heat, on the other hand, there is a great discrepancy between estimated values and the values estimated using the energy balance equation, in particular immediately after watering. A plausible reason for this may be the occurrence of convection as a result of watering. We can see from

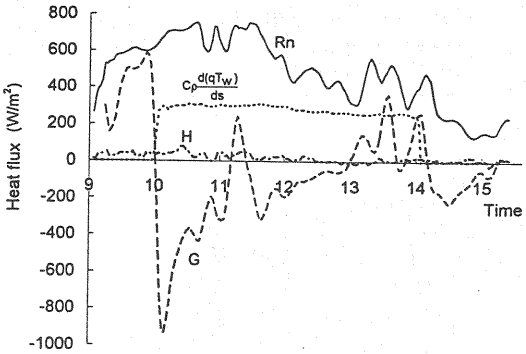

Figure 15. Energy balance at Site A

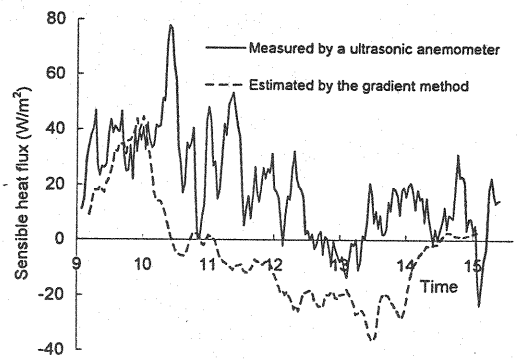

Figure 16. Measured and estimated values of sensible heat

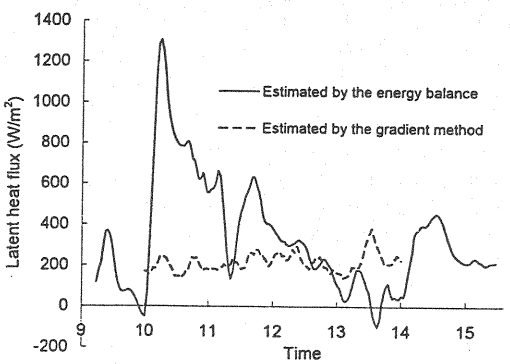

Figure 17. Estimated values of latent heat

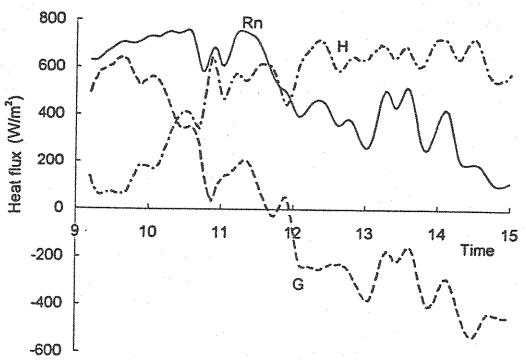

Figure 18. Energy balance at Site B

Figure 17 that the latent heat flux estimated from the energy balance equation gradually decreased after watering and increased again after the termination of watering. This was likely the result of advection caused by the water flowing toward the street drains. On the basis of these results, the data shown in Figures 15, 16 and 17 are believed to be indicative of actual conditions in terms of general tendencies and the quantity of heat except for the time immediately after watering, although there remains uncertainty in the measurement of the heat flux into the ground.

The energy balance at Site B is shown in Figure 18. As was the case with Site A, correction was applied to the heat flux into the ground. According to Figure 18, the sensible heat was 600 W/m^2 or greater at around noon when the net radiation started to decrease, since G had already turned negative. Nevertheless, since the time when heat conduction into the ground becomes negative is, in general, around 3:00 p.m.[2], the reliability of the corrected value of G may require reconfirmation.

Comparing the values of sensible heat and heat flux into the ground at Sites A and B, we can see that they are roughly in the same level between the two sites until the watering commenced. However, the fluctuation of these values for each of the sites is quite different during the watering due to the conveyance of a huge amount of heat in the forms of latent heat and advection. Nevertheless, the difference in temperature between the two sites was not as great as expected due to the effect of the wind blowing from Site A toward Site B.

EFFECT OF WATERING FOR IMPROVING THE THERMAL ENVIRONMENT

The effect of watering for improving the thermal environment is evaluated below, based on a discomfort index and thermal load calculated using the measured data. The discomfort index is a thermal index for indoor environments which accounts for the

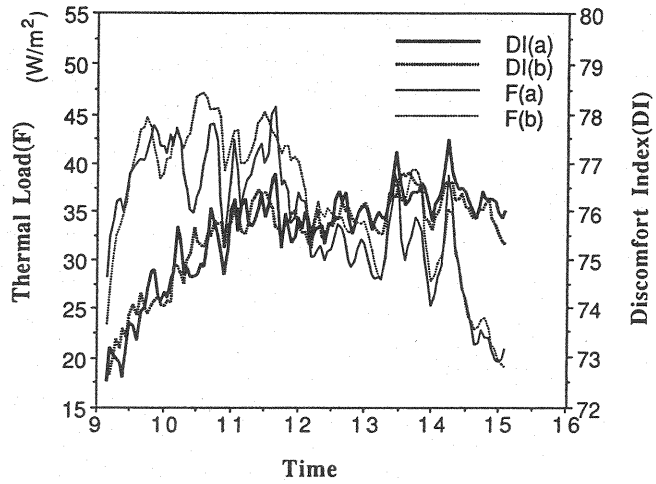

Figure 19. Time distribution of thermal indices

effect of temperature and humidity, while thermal load is the net amount of heat which a human hypothetically receives from his surroundings. In other words, the latter is considered to be a thermal index for outdoor environments in which temperature, humidity, wind and radiation are taken into consideration.

The discomfort index (DI) was calculated by eq. (5) below[3]:

$$DI = 0.81T_a + 0.01Rh(0.99T_a - 14.3) + 46.3 \quad (5)$$

where T is air temperature (°C), and Rh is relative humidity (%).The thermal load (F) on a human is defined by eq. (6):

$$F = R + M - r - C - \ell E \quad (6)$$

where R is the heat received by radiation, M is the metabolic rate of a human, r is the long-wave radiation from a human to the air, C is the convective heat flux, and ℓE is the latent heat. Each term in eq. (6) is estimated after Kanda and Tsuchiya[4], assuming human skin temperature to be constant.

Figure 19 shows the results of the discomfort index and the thermal load during the measurement. Although the watering caused almost no difference in the discomfort index, it reduced the thermal load by around 10 W/m^2. Assuming that this amount only concerns an increase in sensible heat from a naked body (i.e., an increase in the skin temperature), the skin temperature may rise by about 1.5 degrees. Thus, although the watering may not be effective enough to improve indoor heat environments, it is quite effective for reducing the thermal load in the canopy constituted by road surfaces and buildings.

CONCLUSION

The experiment of watering in an urban area proved the following: 1) Watering caused unequivocal differences in air temperature, globe temperature and relative humidity between two sites at a short distance, one watered and the other not; 2) Since the use of groundwater produced a great effect in heat absorption and advection, an increase in humidity was successfully suppressed; and 3) Roadway watering was proved effective for moderating thermal environments, since it prevented an increase in the temperature of the road surface.

In areas already equipped with snow-melting pipes, the introduction of watering as a countermeasure against intense heat in summer is comparatively easy, provided annoyance to traffic and pedestrians, and stability of the water supply are taken

into consideration. Even in areas where such pipes have not yet been installed, however, watering may be introduced if the cost-effectiveness for the watering is proved.

ACKNOWLEDGMENTS

The authors would like to express their deep gratitude to Mr. Shimatani of the River Environment Division of Public Works Research Institute for valuable suggestions, as well as the Shinanogawa Work Office of the Ministry of Construction and the Engineering Department of Nagaoka City, for their warm cooperation in conducting the field observation. Finally, the authors would be proud to note that part of this study was supported by a Grant-in-Aid for Developmental Scientific Research from the Ministry of Education, Science and Culture of Japan.

REFERENCES

1) Kanda, M., T. Abe and M. Hino : A study on the watering effect as a preventive measure against the heat island phenomenon, Proc. of 1993 Conference of Japan Society of Hydrology and Water Resources. (in Japanese)

2) Asaeda, T. and T. Fujino : Heat flux and heat storage properties of the paved ground, Journal of Japan Society of Hydrology and Water Resources, Vol.5, No.4, pp.3-7, 1992. (in Japanese)

3) Chronological Table of Science, p. 266, 1992. (in Japanese)

4) Kanda, M. and N. Tsuchiya : Field observation and analysis for estimating thermal load on a human body, 38th Japanese Conference on Hydraulics, pp.419-424, 1994. (in Japanese)

APPENDIX - NOTATION

The following symbols are used in this paper:

- $c\rho$ = heat capacity of water;
- C = convective heat flux;
- E = rate of evaporation;
- F = thermal load on a human body;
- G = heat flux into the ground;
- H = sensible heat flux into the atmosphere;
- ℓE = latent heat flux into the atmosphere;
- $L\downarrow$ = downward long-wave radiation;
- M = metabolic rate;
- q = discharge per unit width of the road;
- r = long-wave radiation from a human to the air;
- R = heat received by radiation;
- Rh = relative humidity;
- R_n = net radiation;
- s = distance along the flow direction of sprinkled water;
- $S\downarrow$ = downward short-wave radiation;
- $S\uparrow$ = upward short-wave radiation;
- T = ground surface temperature;
- T_a = air temperature;
- T_w = water temperature; and
- σ = Stefan-Boltzmann constant, respectively.

(Received January 20, 1995; revised December 19, 1996)